3DC-Cobotic Manipulator

Sirisak Sirikasemsuk, and Witaya Wannasuphoprasit*
Department of Mechanical Engineering
Chulalongkorn University
Phayathai Rd, Pathum Wan Bangkok 10330 Thailand
Sirisak.S@gmail.com, witaya.w@chula.ac.th*
*corresponding author

Abstract

The 3DC-Cobotic Manipulator is a passive robot designed for direct collaboration with a human operator. This Cobot utilizes three wheel CVTs to control the rotational axis of a sphere. The sphere's motion is then transmitted to linear motions in Cartesian space via a serial manipulator. Design and construction of the Cobot prototype is described in detail. The kinematics of the 3DC-Cobotic Manipulator is divided into five spaces: configuration space, joint space, spherical space, coupling space, and steering space. The transformations of these spaces are provided, and simulation motion was performed to verify the overall kinematics of the Cobot. The Control structure of the Cobot consists of feedforward and feedback controls. We performed two path experiments using this controller. In the first experiment, an operator moved the end-effector along a vertical straight line. Then in the second experiment the operator moved the end-effector back and forth along a circular reference path. The experimental results show the controller can reduce error, and achieve satisfactory track reference paths.

Keywords: Cobot, Kinematics, Passive

1. Introduction

A Cobot (collaborative robot) is one of a class of passive robots designed to interact directly with a human operator. The first Cobot was developed by W. Wannasuphoprasit et al. [2, 3].

Cobots are intrinsically passive, and thus safe for an operator to work with within a shared workspace. Cobots generate programmable reference paths, so-called virtual guidances, which guide and assist humans in performing motion tasks.

In general a regular robot can create virtual guidance as well. Consider Fig. 1. The robot controls joint movement and uses power from an actuator to create motions. When interacting with humans, this active power from the robot can be transmitted to human operators, and thus impose serious concerns for human safety. If anything goes wrong (i.e. a controller fails or a sensor malfunctions) the robot can move and potentially harm human operators.

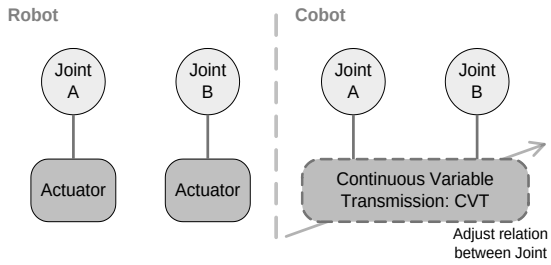

Fig. 1 Comparison of a robot and a Cobot

In contrast to a robot that controls a joint directly, a Cobot controls the relations between joints. Cobots utilize CVT, continuous variable transmission, to connect two joints together. Thus, the direction of

motion can be controlled by varying the transmission ratio. This structure makes Cobots inherently passive and guarantees safety, because a Cobot cannot move by itself.

In order to control any direction of motion, the Cobot's CVT must have the following properties:

- Infinite transmission ratio with zero value
- The transmission ratio can be adjusted to positive and negative ranges

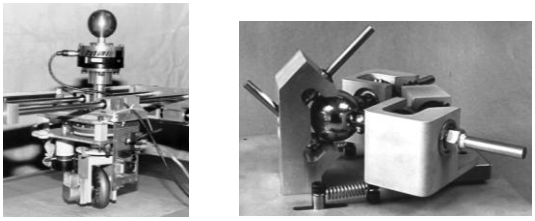

(a) (b)

Fig. 2 (a) linear velocity CVT; (b) angular velocity CVT

Up to the present, two types of CVT have been used extensively in Cobots. The first is linear velocity CVT, and the second is angular velocity CVT.

This work focuses on the linear velocity CVT shown in Fig. 3. Linear velocity CVT consists of a wheel and a steering motor. The wheel is the simplest CVT that couples velocities in x and y directions in a plane. The transmission ratio of linear velocity CVT can be easily found as:

$$\tan\phi = \frac{\dot{y}}{\dot{x}},$$

where ϕ is the steering angle, and $\dot{x}$ and $\dot{y}$ are velocities in the x and y directions, respectively. For example, if ϕ = 0°, $\vec{V} = v_x$, and the wheel will roll in the x direction. The transmission ratio can be simply set by varying the steering angle.

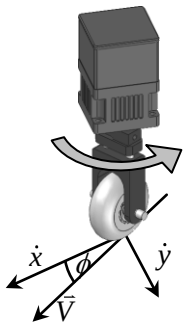

Fig. 3 Linear velocity CVT

An example of a Cobot that uses wheel linear CVTs is the Scooter Cobot [3] depicted in Fig. 4. Scooter is a planar Cobot that has three degrees of freedom (DOF) in x,y,θ space. It consists of three wheel joints installed in parallel.

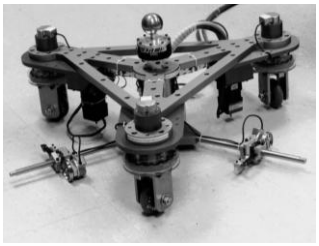

Fig. 4 Scooter Cobot

When interacting with a human operator, Scooter directs the operator's motion through virtual guidance by controlling the steering angles of all wheels. Scooter is very simple and effective. However, it is only able to operate on a plane. Since most applications require 3D Cartesian workspace, this work focuses on the development of a Cobot that has the capability to function in such a workspace.

2. 3DC-Cobot concept

Our purpose is to develop a Cobotic manipulator that operates in Cartesian space. This prototype will be used to explore Cobot applications and study control of a passive haptic interface. The prototype is aimed for laboratory uses, with

a workspace of about 1.5 ft^3.

Several Cobotic prototypes that have been developed have complicated structures, and most of them require spherical CVTs [4,5,7]. We selected the wheel joints in our design due to their simplicity.

The key idea of the 3DC-Cobot was developed from the architecture of Scooter. Scooter has three wheel joints installed on the base. All wheel CVT joints move together with the Cobot's body as a rigid frame. Since we use the Earth as an inertial frame, the Earth stays still while the Scooter rolls and moves.

Imagine if we radically reduce the size of the Earth to a small sphere, and we place the sphere on a stationary wheel CVT base as shown in Fig. 5(b). Here the motion of the sphere can be controlled by steering the wheel angles.

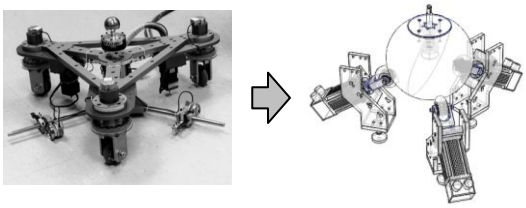

Scooter Cobot (a)

3D-Cobot (b)

Fig. 5 The concept of a 3DC-Cobot

Since the sphere's motion consists of roll, pitch and yaw, a linkage mechanism is needed to transmit this rotational movement to linear motions in Cartesian space. This can be easily done by attaching a manipulator on top of the sphere. The roll and pitch motions will be naturally transformed into translational motions, just like a joystick. The yaw or spinning motion of the sphere requires a special transmission design. Details of the linkage, mechanism and transmission will be presented in the next section.

3. 3DC-Cobot Manipulator prototype

Detailed design

This section describes the design and construction of the Cobot prototype. The 3DC-Cobot Manipulator consists of several main parts: 1) a station base; 2) three wheel joints; 3) a sphere; 4) a serial arm; and 5) a cable transmission and preload mechanism.

The wheel joint comprises a commercial polyurethane wheel and a steering motor. (To simplify we use the motor directly without a transmission.)

The wheel joints are purposely configured so that their axes intersect at the center of the sphere. All axes are at 90° angles to each other to form orthogonal axes, as shown in Fig. 6.

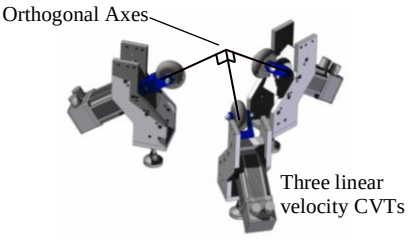

Fig. 6 Three linear CVTs lie on three orthogonal axes

The base serves as a key structure for the Cobot. All wheel joints are rigidly connected to the base.

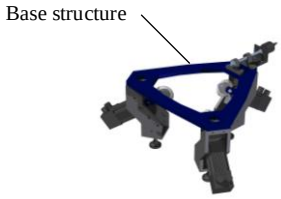

Fig. 7 The station base with three wheel joints installed

In this work, a bowling ball is used as the sphere, because it provides good sphericity, with a smooth surface finish. The sphere is positioned directly on three wheels. The sphere can rotate around any

axis of rotation, but cannot translate.

Consider the sphere in Fig. 8. We modified the sphere and installed a linear hub with stiff spring inside. The spring preload force applied on the sphere ensures positive contact between the wheels and the sphere's surface.

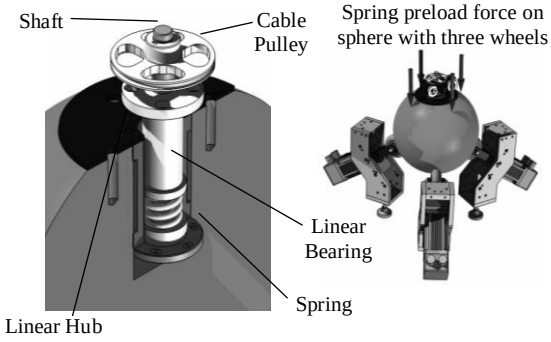

Fig. 8 Spring Preload Mechanism

A shaft is installed inside the linear hub. This shaft translates and rotates with the sphere. Note that it can slide up and down with a linear bearing in the linear hub. A cable pulley is fixed on top of the shaft. The pulley acts as a yaw transmission, which will be explained later.

Since all rotational motions of the sphere will be converted to Cartesian space, a three-joint arm is installed for this purpose. Recall that the roll and pitch motions will be converted directly by a spherical joint, and the yaw motion will be converted through an additional link joint via a transmission.

After a thorough design review, we selected a concentric multilink spherical (CMS) joint, developed by Hamlin and Sanderson [1]. As shown in Fig. 9, this multilink spherical joint is compact and easy to manufacture.

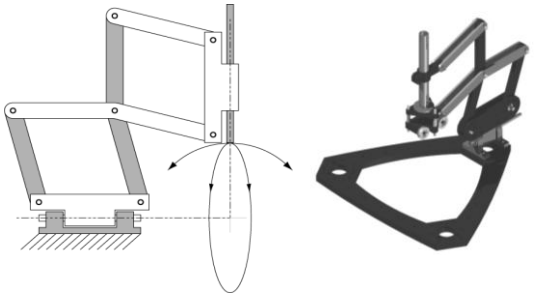

Fig. 9 Concentric multilink spherical (CMS) joint

The sphere's roll and pitch motions are now connected directly to the CMS joint mechanism. The CMS joint increases the stiffness of the structure.

In order to transfer the yaw motion, we placed an additional elbow joint and linkage at the CMS joint, as shown in Fig. 10. Furthermore we added a cable transmission to convert the yaw motion of the sphere to the elbow joint via the cable pulley. The transmission ratio is equal to 2. Details of the cable transmission are shown in Fig. 10(b).

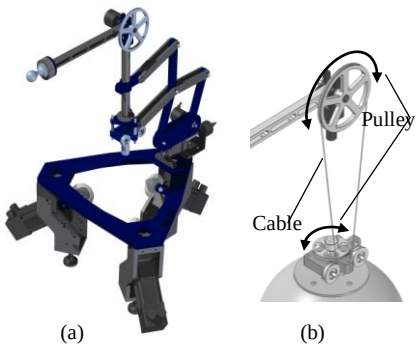

Fig. 10 a) the complete serial arm;
b) cable transmission converts yaw to elbow motion

The serial arm of the 3D-Cobot is an anthropomorphic arm. It has three joints. The first and second joint axes intersect at the center of the sphere. The third joint is placed parallel to the second joint. The link lengths of the serial arms are 400 mm and 250 mm, respectively. The complete design

of the 3DC-Cobot Manipulator is presented in Fig. 11.

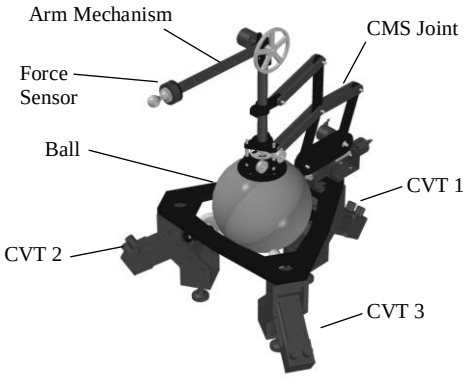

Fig. 11 A CAD model of the 3D-Cobot

Figs. 12-14 display roll-pitch-yaw motions of the sphere and corresponding motions of the serial arm in Cartesian space. The details of mapping will be provided in the next section.

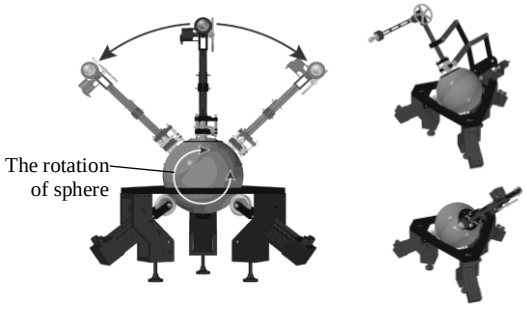

Fig. 12 Roll motion and arm movement

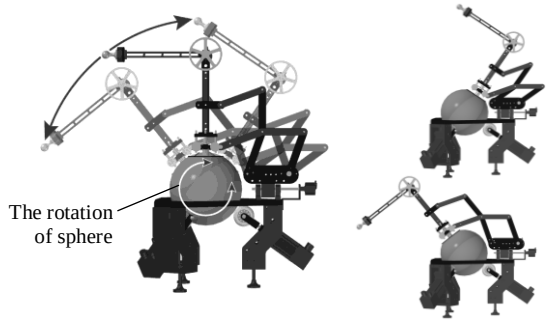

Fig. 13 Pitch motion and arm movement

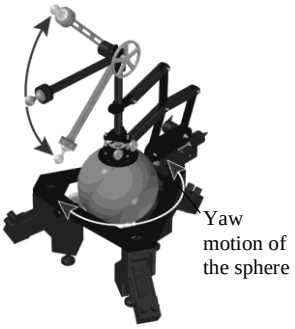

Fig. 14 Yaw motion and elbow movement

Prototype construction

Most of the base structures are made from anodized aluminum. For wheel joints, we selected brushless servo motors to steer the wheels. All joints in the serial arm are equipped with optical encoders. The transmission cable is made from stainless steel. We used a screw tensioner to tighten the cable. Fig. 15(a) shows this cable-pulley transmission. The CMS joints are made from aircraft-grade aluminum alloy. Each component was machined by computer numerical control (CNC) to control joint positions and tolerances.

(a) (b)

Fig. 15 (a) cable-pulley transmission; (b) CMS joint

Fig. 16 shows the complete prototype of the 3DC-Cobot Manipulator.

Fig. 16 The 3DC-Cobot Manipulator

4. Kinematics

The 3DC-Cobot Manipulator consists of several linkages that transform spherical motion to a serial link manipulator, as described previously.

Kinematics analysis of the Cobot can be presented in terms of space [5,6] by dividing the overall kinematics into: configuration space (C_T), joint space (C_J), spherical space (C_{Sp}), coupling space (Σ_i), and steering space (Φ_i).

A. Configuration Space (C_T)

Configuration space (or "task space") of the 3DC-Cobotic Manipulator is the linear Cartesian space shown in Fig. 17.

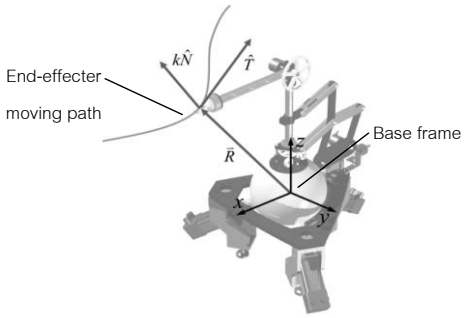

Fig. 17 Configuration space

The end-effector's movement of the 3DC-Cobotic Manipulator is measured relative to the base frame. The origin of the base frame is set at the center of the sphere where all wheel axes intersect. The position vector ($\vec{R}$) of the end-effector can be defined as:

$$\vec{R} = \begin{bmatrix} x & y & z \end{bmatrix}^T, \quad (1)$$

where x, y and z are components in the x, y and z axes, respectively.

Physical architecture of the Cobot consists of continuous variable transmissions, CVTs, which require steering control. Therefore the Cobot's kinematics is derived from position vector ($\vec{R}$), to tangent vector ($\hat{T}$), to curvature vector ($k\hat{N}$), and to steering velocity.

In addition, working collaboratively, a human controls and applies motion while the Cobot controls the direction. Thus, it is suitable to derive the kinematics based on path length parameter.

The tangent vector is a unit vector defined as:

$$\hat{T} = \frac{d\vec{R}}{ds} = \frac{\vec{V}}{|\vec{V}|} \quad (2)$$

where s is path length, and $\vec{V}$ is the velocity vector.

The curvature vector ($k\hat{N}$) has two components: k, the curvature magnitude of the path; and $\hat{N}$, the normal vector. Its direction points to the instantaneous center of rotation. The curvature vector is defined as:

$$k\hat{N} = \frac{d\hat{T}}{ds} \quad (3)$$

These vectors are then transformed via adjacent spaces.

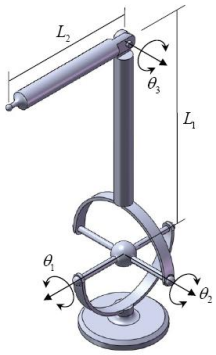

Fig. 18 Joint parameters

B. Joint Space (C_J)

Joint space is the space for describing joint motion, as shown in Fig. 18. All joint positions of the Cobot are measured from the encoders.

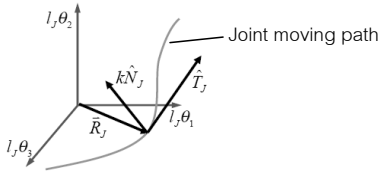

Fig. 19 Joint space

Similar to the configuration space, the position vector ($\vec{R}_J$) in joint space can be written as:

$$\vec{R}_J = \begin{bmatrix} l_J\theta_1 & l_J\theta_2 & l_J\theta_3 \end{bmatrix}^T \tag{4}$$

Here, without losing generality, angular positions ($\theta_1, \theta_2, \theta_3$) are multiplied by the unit length parameter (l_J). The $\vec{R}_J$ in joint space is displayed in Fig. 19.

The forward kinematics is demonstrated by the function $\vec{R} = L\left(\vec{R}_J\right)$. Thus we can write:

$$\vec{R} = \begin{bmatrix} x \\ y \\ z \end{bmatrix} = \begin{bmatrix} L_2\cos\left(\theta_2+\theta_3\right) - L_1\sin\theta_2 \\ L_2\sin\theta_1\sin\left(\theta_2+\theta_3\right) + L_1\sin\theta_1\cos\theta_2 \\ L_2\cos\theta_1\sin\left(\theta_2+\theta_3\right) + L_1\cos\theta_1\cos\theta_2 \end{bmatrix} \tag{5}$$

where L_1, L_2 are the lengths of the first and second links, respectively, as indicated in Fig. 18.

The inverse relation $\vec{R}_J = L_J\left(\vec{R}\right)$ can be written as:

$$\vec{R}_J = \begin{bmatrix} l_J\theta_1 \\ l_J\theta_2 \\ l_J\theta_3 \end{bmatrix} = l_J \begin{bmatrix} A\tan 2\left(y,z\right) \\ 2\cdot A\tan 2\left(-x \pm \sqrt{a^2+x^2-b^2}, a+b\right) \\ 2\cdot A\tan 2\left(L_2 \pm \sqrt{{L_2}^2-c^2}, c\right) \end{bmatrix} \tag{6}$$

where

$$a = \sqrt{y^2+z^2}\ , b = \frac{1}{2L_1}\left(x^2+y^2+z^2+{L_1}^2-{L_2}^2\right),$$

$$c = \frac{1}{2L_1}\left(x^2+y^2+z^2-{L_1}^2-{L_2}^2\right)$$

Here, the tangent vector of configuration space can be transformed to the tangent vector of joint space as:

$$\hat{T}_J = \frac{\mathbf{J}_J\hat{T}}{\left|\mathbf{J}_J\hat{T}\right|}, \tag{7}$$

where $\mathbf{J}_J = \dfrac{\partial L_J}{\partial \vec{R}}$ is a Jacobian matrix. From Equation (6) $\mathbf{J}_J$ can be written as:

$$\mathbf{J}_J = \begin{bmatrix} \dfrac{\partial\theta_1}{\partial x} & \dfrac{\partial\theta_1}{\partial y} & \dfrac{\partial\theta_1}{\partial z} \\ \dfrac{\partial\theta_2}{\partial x} & \dfrac{\partial\theta_2}{\partial y} & \dfrac{\partial\theta_2}{\partial z} \\ \dfrac{\partial\theta_3}{\partial x} & \dfrac{\partial\theta_3}{\partial y} & \dfrac{\partial\theta_3}{\partial z} \end{bmatrix}. \tag{8}$$

All elements are listed as follows:

$$\frac{\partial\theta_1}{\partial x} = 0$$

$$\frac{\partial\theta_1}{\partial y} = \frac{z}{y^2+z^2} = \frac{z}{a^2}$$

$$\frac{\partial\theta_1}{\partial z} = \frac{-y}{y^2+z^2} = \frac{-y}{a^2}$$

$$\frac{\partial\theta_2}{\partial x} = \frac{L_1xc - xr^2}{L_1r^2\sqrt{r^2-c^2}} - \frac{a}{r^2}$$

$$\frac{\partial\theta_2}{\partial y} = \frac{L_1yc - yr^2}{L_1r^2\sqrt{r^2-c^2}} + \frac{xy}{ar^2}$$

$$\frac{\partial\theta_2}{\partial z} = \frac{L_1zc - zr^2}{L_1r^2\sqrt{r^2-c^2}} + \frac{xz}{ar^2}$$

$$\frac{\partial\theta_3}{\partial x} = \frac{x}{L_1\sqrt{L_2{}^2 - d^2}}$$

$$\frac{\partial\theta_3}{\partial y} = \frac{y}{L_1\sqrt{L_2{}^2 - d^2}}$$

$$\frac{\partial\theta_3}{\partial z} = \frac{z}{L_1\sqrt{L_2{}^2 - d^2}}$$

where

$$a = \sqrt{y^2 + z^2}\ ,$$

$$b = \frac{\left(x^2 + y^2 + z^2 + L_1{}^2 - L_2{}^2\right)}{2L_1},$$

$$c = \frac{\left(x^2 + y^2 + z^2 - L_1{}^2 - L_2{}^2\right)}{2L_1},\ r^2 = x^2 + y^2 + z^2$$

Next, the curvature transformation from the configuration space ($k\hat{N}$) to the curvature vector of joint space can be expressed as:

$$k_J\hat{N}_J = \frac{\left[\mathbf{I} - \hat{T}_J\hat{T}_J{}^T\right]}{\left|\mathbf{J}_J\hat{T}\right|^2}\left[\hat{T}^T\begin{bmatrix}\mathbf{H}_{J1}\\ \mathbf{H}_{J2}\\ \mathbf{H}_{J3}\end{bmatrix}\hat{T} + \mathbf{J}_J k\hat{N}\right] \qquad (9)$$

where $\mathbf{H}_{J1}, \mathbf{H}_{J2}, \mathbf{H}_{J3}$ are the Hessian matrix defined as: $\mathbf{H}_{Ji} = \frac{\partial^2 L_{Ji}}{\partial\bar{R}^2}$, $i = 1, 2, 3$ as detailed in the Appendix.

C. Spherical space (C_{Sp})

Here we define spherical space as a rotation space consisting of rotational components in X, Y and Z axes, as shown in Fig. 20.

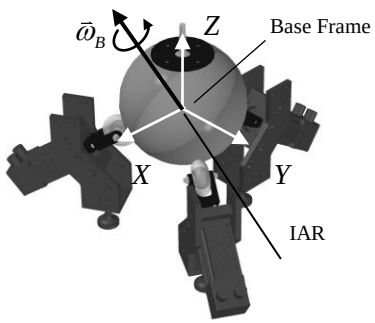

Fig. 20 Spherical space

At any moment in time, the sphere will rotate at an instantaneous axis of rotation (IAR). To express sphere motion, consider a sphere rotating with angular velocity $\bar{\omega}_B$ around the IAR. The $\bar{\omega}_B$ can be described as a product of a Jacobian and joint space velocity vector:

$$\bar{\omega}_B = \begin{bmatrix}\omega_{Bx}\\ \omega_{By}\\ \omega_{Bz}\end{bmatrix} = \begin{bmatrix}-1 & 0 & \rho\sin\theta_2\\ 0 & -\cos\theta_1 & -\rho\sin\theta_1\cos\theta_2\\ 0 & \sin\theta_1 & -\rho\cos\theta_1\cos\theta_2\end{bmatrix}\begin{bmatrix}\dot{\theta}_1\\ \dot{\theta}_2\\ \dot{\theta}_3\end{bmatrix} \qquad (10)$$

where $\omega_{Bx}, \omega_{By}, \omega_{Bz}$ are the components of the angular velocity on the X, Y and Z axes, respectively. Here the 3x3 matrix is the Jacobian matrix J_B. Thus the tangent vector ($\hat{T}_B$) and the curvature can be determined from the equation:

$$\hat{T}_B = \frac{\mathbf{J}_B\hat{T}_J}{\left|\mathbf{J}_B\hat{T}_J\right|}, \qquad (11)$$

and the curvature vector ($k_B\hat{N}_B$) of spherical space determined from the equation:

$$k_B\hat{N}_B = \frac{\partial\hat{T}_B}{\partial S_S} = \frac{\left[\mathbf{I} - \hat{T}_B\hat{T}_B{}^T\right]}{\left|\mathbf{J}_B\hat{T}_J\right|}\left[\hat{T}_J{}^T\frac{\partial\mathbf{J}_B}{\partial\bar{R}_J}\hat{T}_J + \mathbf{J}_B k_J\hat{N}_J\right] \qquad (12)$$

where $\frac{\partial\mathbf{J}_B}{\partial\bar{R}_J} = \mathbf{H}_B$ is the Hessian matrix in spherical space (see Appendix).

D. Coupling space (Σ_i)

Coupling space, in our case, is defined as a rectangular plane that is placed at a wheel-sphere contact point and is perpendicular to the steering axis, as shown in Fig. 21. In a 3DC-Cobotic Manipulator, there are three coupling spaces (equal to the number of CVTs).

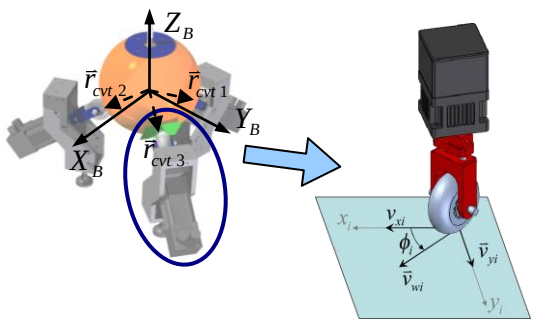

Fig. 21 The coupling space of linear velocity CVT

When the sphere rotates, the wheel-sphere contact point has the relative velocity $\vec{v}_{wi}$. The velocity components on the coupling space, $\vec{v}_{xi}$ and $\vec{v}_{yi}$, have a transmission ratio set by the wheel steering angle. $\vec{v}_{wi}$ on the coupling plane can derived from:

$$\vec{v}_{wi} = \vec{\omega}_B \times \vec{r}_{cvt\,i}, \tag{13}$$

where $\vec{r}_{cvt\,i}$ is the configuration vector of the i[th] CVT, as depicted in Fig. 21. Equation (15) can be described as:

$$\vec{v}_{wi} = \begin{bmatrix} v_{xi} \\ v_{yi} \end{bmatrix} = \begin{bmatrix} -r_{ball}a_2 & -r_{ball}b_2 & -r_{ball}c_2 \\ r_{ball}a_1 & r_{ball}b_1 & r_{ball}c_1 \end{bmatrix}_i \begin{bmatrix} \omega_{Bx} \\ \omega_{By} \\ \omega_{Bz} \end{bmatrix} \tag{14}$$

where r_{ball} is the radius of the sphere. Note that the 2x3 matrix is the Jacobian matrix $\mathbf{j}_{wi}$ that relates the rate of change in the spherical space to the coupling space. Here all elements in $\mathbf{j}_{w1}$, $\mathbf{j}_{w2}$ and $\mathbf{j}_{w3}$ are described below as:

$$\mathbf{j}_{w1} = r_{ball}\begin{bmatrix} -\frac{1}{\sqrt{6}} & \frac{1}{\sqrt{2}} & \frac{1}{\sqrt{3}} \\ \frac{1}{\sqrt{6}} & \frac{1}{\sqrt{2}} & -\frac{1}{\sqrt{3}} \end{bmatrix},$$

$$\mathbf{j}_{w2} = r_{ball}\begin{bmatrix} -\frac{1}{\sqrt{6}} & -\frac{1}{\sqrt{2}} & \frac{1}{\sqrt{3}} \\ -\sqrt{\frac{2}{3}} & 0 & -\frac{1}{\sqrt{3}} \end{bmatrix},$$

and

$$\mathbf{j}_{w3} = r_{ball}\begin{bmatrix} \sqrt{\frac{2}{3}} & 0 & \frac{1}{\sqrt{3}} \\ \frac{1}{\sqrt{6}} & -\frac{1}{\sqrt{2}} & -\frac{1}{\sqrt{3}} \end{bmatrix}$$

respectively.

Then the tangent vector ($\hat{t}_{wi}$) is determined from:

$$\hat{t}_{wi} = \frac{\mathbf{j}_{wi}\hat{T}_B}{\left|\mathbf{j}_{wi}\hat{T}_B\right|} \tag{15}$$

The curvature vector ($k_{wi}\hat{n}_{wi}$) of each coupling space is expressed as:

$$k_{wi}\hat{n}_{wi} = \frac{\left[\mathbf{I} - \hat{t}_{wi}\hat{t}_{wi}^{\,T}\right]}{\left|\mathbf{j}_{wi}\hat{T}_B\right|}\left[\mathbf{j}_{wi}k_B\hat{N}_B\right] \tag{16}$$

E. Steering velocity

The transmission ratio (Tr_i) and steering angle (ϕ_i) are related as:

$$Tr_i = \frac{v_{yi}}{v_{xi}} = \tan(\phi_i) \tag{17}$$

To steer each wheel, the steering velocity can be determined as:

$$\dot{\phi} = u_i k_{wi} \quad i = 1,2,3 \tag{18}$$

where u_i is the i[th] wheel's rolling speed.

Summary of 3D-Cobot kinematics

The kinematics transformation of all spaces is depicted in Fig. 22. There are four inputs in the system: position vector ($\bar{R}$), tangent vector ($\hat{T}$), curvature vector ($k\hat{N}$), and speed. These configuration parameters are transformed through each space, and the outcome is the steering angular velocity ($\dot{\phi}_i$).

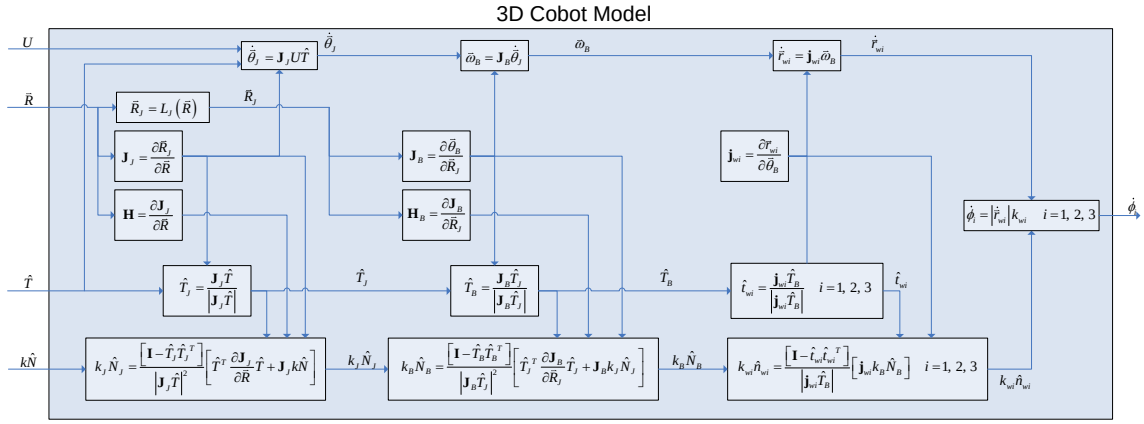

Fig. 22 Diagram of 3DC-Cobotic Manipulator kinematics

5. Controller

In this paper, we are interested in the Cobot constraint on the human movement along the preprogrammed path. Since this Cobot utilizes friction based CVTs, in a real situation the positioning error occurs due to slip. Another error comes from tangential inaccuracy. Figure 23 displays typical reference and actual paths, where $\vec{R}$ and $\hat{T}$ are the actual position and tangent vectors, and $\vec{R}_P$ and $\hat{T}_P$ are the plane position and tangent vectors.

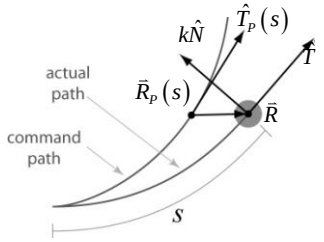

Fig. 23 Configuration error

The control of the 3DC-Cobotic Manipulator consists of feedforward and feedback terms. The control structure uses a similar principle to one previously developed by Wannasuphoprasit et al. [3]. The aim of the controller is to reduce position error and direction error.

Feedforward control provides fast time response, and is implemented according to the kinematics transformation. It implies that feedforward control of Cobot approximates the position ($\vec{R}_P$) and direction ($\hat{T}_P$) of the end-effector on the designated path under the command of the curvature vector ($k\hat{N}$).

Feedback control compensates for positioning and tangent error. The positioning term minimizes path error, while tangential feedback provides smooth operation. Both gains must be experimentally tuned to provide the best result. The modified command curvature for the Cobot is expressed as:

$$k_c\hat{N}_c = k_P\hat{N}_P - \left(G_R\Delta\vec{R} + G_T\Delta\hat{T}\right), \qquad (19)$$

where the command curvature vector, $k_c\hat{N}_c$ is the combination of the feedforward command ($k_P\hat{N}_P$) and the feedback command $-\left(G_R\Delta\vec{R} + G_T\Delta\hat{T}\right)$ as shown in Fig. 24, and G_R and G_T are the positioning and tangential gains, respectively.

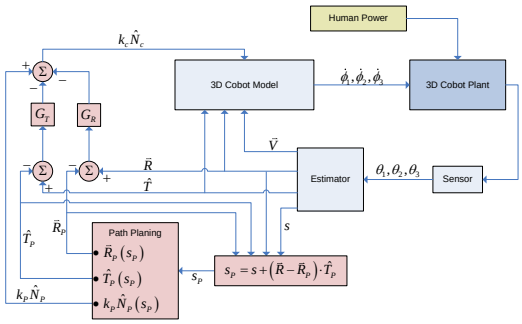

Fig. 24 Block diagram showing the controller and the Cobot model

Details of the Cobot's control implementation can be found in [3]. The control diagram of the 3DC-Cobotic Manipulator is shown in Fig. 24. When sensors on the Cobot measure all joint angles, the Estimator estimates their position, direction, velocity, and distance on the configuration space in order to calculate the command curvature as shown in Equation 23. After that, these commands are sent to the block 3DC-Cobot model in Fig. 24.

In operation, an operator applies force to move the Cobot, while the controller controls the direction.

6. Simulation and experiments

The 3DC-Cobotic Manipulator prototype was tested with the path tracking mode. The end-effector was pushed by an applied force from an operator and 3DC-Cobot controller must constrain the end-effector to move along to the reference path that was created at the early stage by computer programming. These verifications were started with computational simulations and practical experiments.

Prior to operating the 3DC-Cobotic Manipulator prototype, we simulated the overall kinematics and control. The reference path is a circular line on the X-Z plane with radius of 100 mm. The end-effector started on the reference path with a tangent error $[-\cos(10.0°)\ 0.0\ -\sin(10.0°)]^T$.

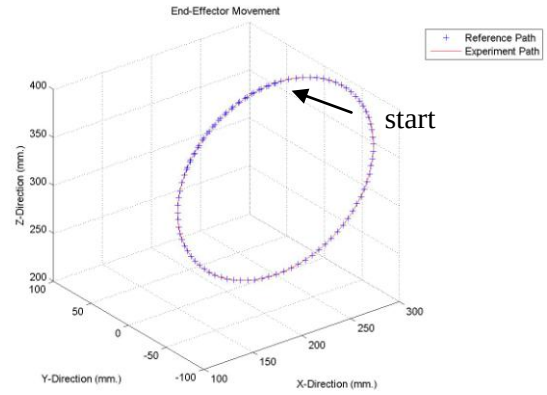

Fig. 25 End-effector movement results from the simulation

Fig. 25 shows the simulation result. The solid line represents the end-effector's trace, and the plus marks represent the reference path. There is no visible error between them. The Cobot tracked along the reference paths fairly well. The corresponding steering angles of all wheels are displayed in Fig. 26.

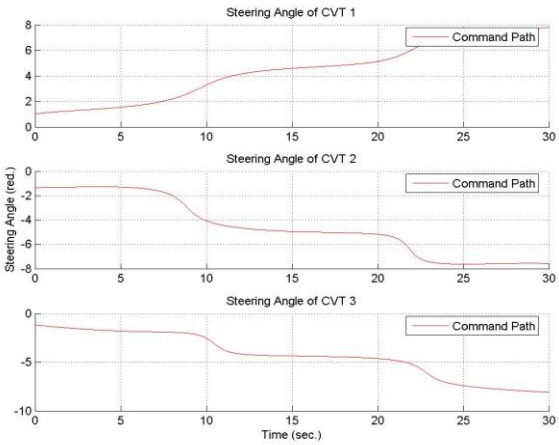

Fig. 26 The steering angle of CVT in the simulation.

The simulation results confirmed the correctness of the existing kinematics. Next we performed experiments on the Cobot prototype using straight and circular paths.

In the first experiment, an operator moved the end-effector along the reference

straight line, as shown in Fig. 27.

At the beginning, the end-effector started with a positioning error from the reference path (about 20 mm). Fig. 28 shows the trace of the end-effector plotted together with the reference path. When the operator moved the end-effector, the controller quickly steered toward, and kept the end-effector well along, the reference path. The steering angles and commands of all three wheels are shown in Fig. 29.

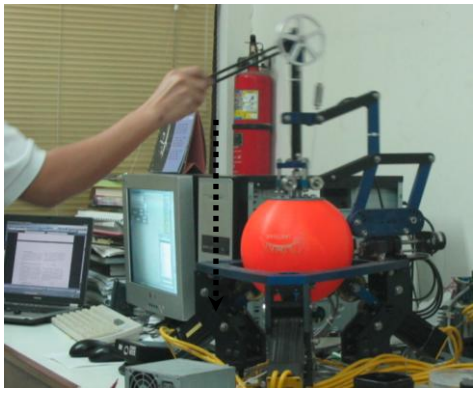

Fig. 27 The steering angle of CVT 1 in the first experiment

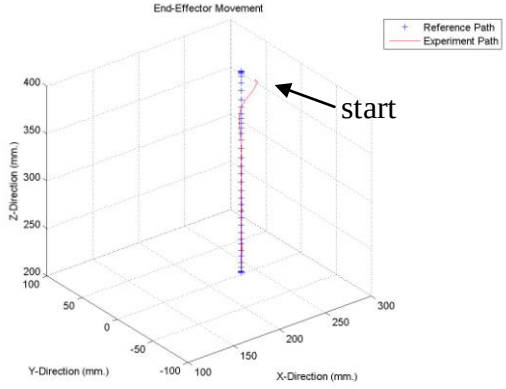

Fig. 28 End-effector movement results from the first experiment

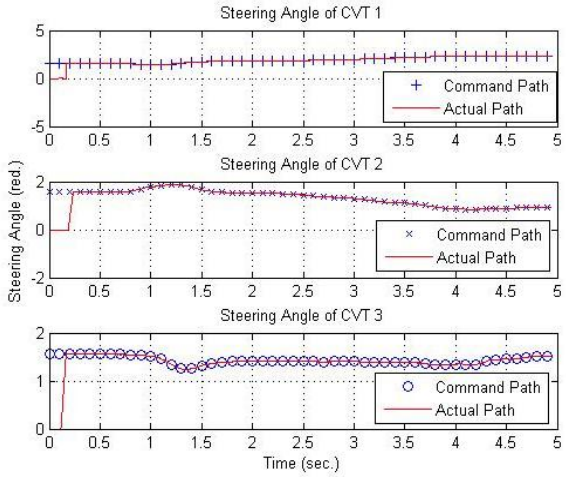

Fig. 29 The steering angle of CVT in the first experiment

In the second experiment, the operator moved the end-effector forward and backward along the circular reference path (with radius of 100 mm). The experimental result is shown in Fig. 30. The controller kept the end-effector along the path with some error. The steering angles and commands of all three wheels are shown in Fig. 31.

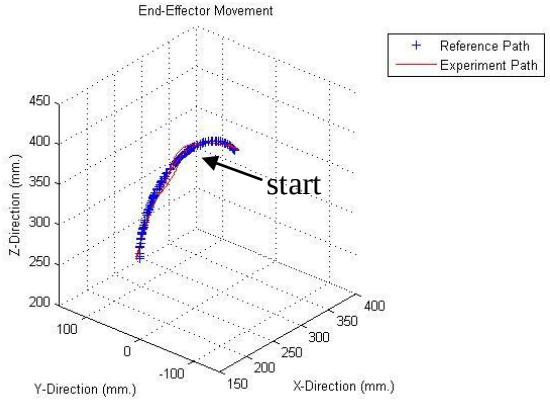

Fig. 30 End-effector movement results from the second experiment

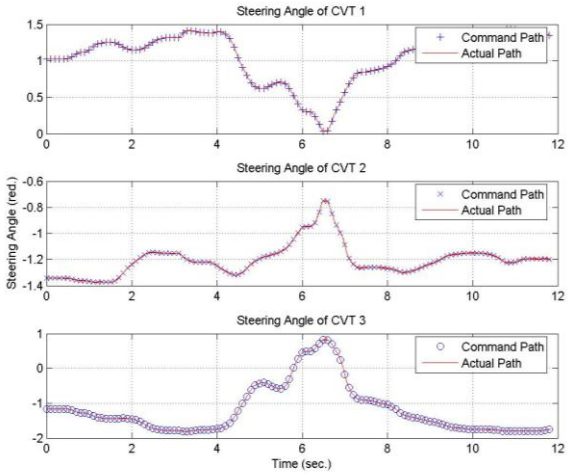

Fig. 31 The steering angle of CVT in the second experiment

7. Conclusion and discussion

This paper presents the design and construction of the 3DC-Cobotic Manipulator using three wheel CVTs. The key mechanism is the CMS manipulator with cable transmission, which converts three sphere rotational motions to three linear motions in the Cartesian workspace.

Kinematics of the Cobot based on path length parameter was described in detail. We derived tangent and curvature transformations of all adjacent spaces: from configuration, to joint, to sphere, to coupling, and to steering spaces. In addition, a simulation of circular motion was performed to verify the kinematics of the Cobot.

The control structure consists of kinematics feedforward together with positioning and tangential feedback controls. The experimental results of the prototype are satisfactory. The controller compensates for slip and tangential error really well. The Cobot tracks the reference path with only small error.

In our experience with the 3DC-Cobotic Manipulator, we found that the spring preload on the sphere must provide high enough force to ensure positive contact of all wheels. Another point of interest is that the tracking performance of the 3DC-Cobotic Manipulator is less than that of the Scooter Cobot, because the aspect ratios of relative motion are less. Recall that a passive Cobot requires some distance to steer toward a target.

8. Acknowledgments

The authors wish to thank the Graduate School of Chulalongkorn University. This work was supported in part by a grant from the National Metal and Material Technology Center, Thailand.

9. References

[1] Gregory J. Hamlin, A. C. Sanderson, A Novel Concentric Multilink Spherical Joint with Parallel, Robotics Applications, IEEE International Conference on Robotics and Automation., Vol. 2, pp. 1267-1272, 1994.

[2] Colgate, J.E., Peshkin, M.A. and Wannasuphoprasit, W., Nonholonomic Haptic Display, IEEE International Conference on, Robotics and Automation. Minneapolis, pp. 539-544, 1996.

[3] W. Wannasuphoprasit, R.B. Gillespie, J.E. Colgate, M.A. Peshkin, Cobot Control, Proceeding of the IEEE 1997 International Conference on Robotics & Automa-tion, pp. 3571-3576, 1997.

[4] C. Moore, Continuously Variable Transmission for Serial Link Cobot Architectures, Master's thesis, Department of Mechanical Engineering, Northwestern University, 1997.

[5] M. Peshkin, J.E. Colgate, P. Akella, W. Wannasuphoprasit, B. Gillespie, C. Moore, Cobot architecture, IEEE Trans. Robot. Automatation. Vol.17 , pp. 377-389, 2001.

[6] R. Brent Gillespie, J. Edward Colgate, Michael A. Peshkin, A General Framework for Cobot Control, IEEE Transactions on Robot-Ics and Automation, Vol. 17, No. 4, 2001.

[7] Carl A. Moore, Michael A. Peshkin, J. Edward Colgate (2002) Cobot Implementation of 3D Virtual Surfaces, Proceedings of the 2002 IEEE International Conference on Robotics &Automation Washington, DC

Sirisak Sirikasemsuk is a Doctor of Engineering candidate and a researcher in the Human Robotics Laboratory, Department of Mechanical Engineering, Chulalongkorn University. He received a Master's degree from Chulalongkorn University

Witaya Wannasuphoprasit is an Assistant Professor in the Mechanical Engineering Department and the director of the Human Robotics Laboratory. He received a Master's Degree and Ph.D from Northwestern University. He received the best paper award from ASME IMECHE 1998, and is a coauthor of the best paper of IEEE ICRA 1996.

10. Appendix

A. Hessian matrix

Joint space:

$$k_J \hat{N}_J = \frac{\left[\mathbf{I} - \hat{T}_J \hat{T}_J{}^T\right]}{\left|\mathbf{J}_J \hat{T}\right|^2} \left[\hat{T}^T \begin{bmatrix} \mathbf{H}_{J1} \\ \mathbf{H}_{J2} \\ \mathbf{H}_{J3} \end{bmatrix} \hat{T} + \mathbf{J}_J k\hat{N} \right],$$

where

$$\mathbf{H}_{J1} = \begin{bmatrix} \frac{\partial^2\theta_1}{\partial x^2} & \frac{\partial^2\theta_1}{\partial x\partial y} & \frac{\partial^2\theta_1}{\partial x\partial z} \\ \frac{\partial^2\theta_1}{\partial y\partial x} & \frac{\partial^2\theta_1}{\partial y^2} & \frac{\partial^2\theta_1}{\partial y\partial z} \\ \frac{\partial^2\theta_1}{\partial z\partial x} & \frac{\partial^2\theta_1}{\partial z\partial y} & \frac{\partial^2\theta_1}{\partial z^2} \end{bmatrix}$$

$$\mathbf{H}_{J2} = \begin{bmatrix} \frac{\partial^2\theta_2}{\partial x^2} & \frac{\partial^2\theta_2}{\partial x\partial y} & \frac{\partial^2\theta_2}{\partial x\partial z} \\ \frac{\partial^2\theta_2}{\partial y\partial x} & \frac{\partial^2\theta_2}{\partial y^2} & \frac{\partial^2\theta_2}{\partial y\partial z} \\ \frac{\partial^2\theta_2}{\partial z\partial x} & \frac{\partial^2\theta_2}{\partial z\partial y} & \frac{\partial^2\theta_2}{\partial z^2} \end{bmatrix}$$

$$\mathbf{H}_{J3} = \begin{bmatrix} \frac{\partial^2\theta_3}{\partial x^2} & \frac{\partial^2\theta_3}{\partial x\partial y} & \frac{\partial^2\theta_3}{\partial x\partial z} \\ \frac{\partial^2\theta_3}{\partial y\partial x} & \frac{\partial^2\theta_3}{\partial y^2} & \frac{\partial^2\theta_3}{\partial y\partial z} \\ \frac{\partial^2\theta_3}{\partial z\partial x} & \frac{\partial^2\theta_3}{\partial z\partial y} & \frac{\partial^2\theta_3}{\partial z^2} \end{bmatrix}$$

And

$$\frac{\partial^2\theta_1}{\partial x^2} = \frac{\partial^2\theta_1}{\partial x\partial y} = \frac{\partial^2\theta_1}{\partial y\partial x} = \frac{\partial^2\theta_1}{\partial x\partial z} = \frac{\partial^2\theta_1}{\partial z\partial x} = 0$$

$$\frac{\partial^2\theta_1}{\partial y^2} = \frac{-2yz}{a^4}$$

$$\frac{\partial^2\theta_1}{\partial y\partial z} = \frac{\partial^2\theta_1}{\partial z\partial y} = \frac{y^2 - z^2}{a^4}$$

$$\frac{\partial^2\theta_1}{\partial z^2} = \frac{2yz}{a^4}$$

$$\frac{\partial^2\theta_2}{\partial x^2}=\left[\left(L_1r^2\sqrt{r^2-c^2}\right)\left(L_1c-x^2-r^2\right)\cdots -\left(L_1xc-xr^2\right)\cdots \frac{3L_1xr^2-2L_1xc^2-xr^2c}{\sqrt{r^2-c^2}}\right]\cdots \Big/\left(L_1r^2\sqrt{r^2-c^2}\right)^2+\frac{2ax}{r^4}$$

$$\frac{\partial^2\theta_2}{\partial x\partial y}=\frac{\partial^2\theta_2}{\partial y\partial x}=\left[-\left(L_1r^2xy\sqrt{r^2-c^2}\right)\cdots -\left(L_1xc-xr^2\right)\cdots \frac{3L_1yr^2-2L_1yc^2-yr^2c}{\sqrt{r^2-c^2}}\right]\cdots \Big/\left(L_1r^2\sqrt{r^2-c^2}\right)^2-\frac{\frac{r^2y}{a}-2ay}{r^4}$$

$$\frac{\partial^2\theta_2}{\partial x\partial z}=\frac{\partial^2\theta_2}{\partial z\partial x}=\left[-\left(L_1r^2xz\sqrt{r^2-c^2}\right)\cdots -\left(L_1xc-xr^2\right)\cdots \frac{3L_1zr^2-2L_1zc^2-zr^2c}{\sqrt{r^2-c^2}}\right]\cdots \Big/\left(L_1r^2\sqrt{r^2-c^2}\right)^2-\frac{\frac{r^2z}{a}-2az}{r^4}$$

$$\frac{\partial^2\theta_2}{\partial y^2}=\left[\left(L_1r^2\sqrt{r^2-c^2}\right)\left(L_1c-y^2-r^2\right)\cdots -\left(L_1yc-yr^2\right)\cdots \frac{3L_1yr^2-2L_1yc^2-yr^2c}{\sqrt{r^2-c^2}}\right]\cdots \Big/\left(L_1r^2\sqrt{r^2-c^2}\right)^2\cdots +\frac{ar^2x-xy\left(2ay+\frac{r^2y}{a}\right)}{\left(ar^2\right)^2}$$

$$\frac{\partial^2\theta_2}{\partial y\partial z}=\frac{\partial^2\theta_2}{\partial z\partial y}=\left[-\left(L_1r^2yz\sqrt{r^2-c^2}\right)\cdots -\left(L_1yc-yr^2\right)\cdots \frac{3L_1zr^2-2L_1zc^2-zr^2c}{\sqrt{r^2-c^2}}\right]\cdots \Big/\left(L_1r^2\sqrt{r^2-c^2}\right)^2\cdots -\frac{xy\left(\frac{zr^2}{a}+2za\right)}{\left(ar^2\right)^2}$$

$$\frac{\partial^2\theta_2}{\partial z^2}=\left[\left(L_1r^2\sqrt{r^2-c^2}\right)\left(L_1c-z^2-r^2\right)\cdots -\left(L_1zc-zr^2\right)\cdots \frac{3L_1zr^2-2L_1zc^2-zr^2c}{\sqrt{r^2-c^2}}\right]\cdots \Big/\left(L_1r^2\sqrt{r^2-c^2}\right)^2\cdots +\frac{axr^2-xz\left(\frac{zr^2}{a}+2za\right)}{\left(ar^2\right)^2}$$

$$\frac{\partial^2\theta_3}{\partial x^2}=\frac{L_1\left(L_2{}^2-d^2\right)+x^2d}{L_1{}^2\left(L_2{}^2-d^2\right)^{3/2}}$$

$$\frac{\partial^2\theta_3}{\partial x\partial y}=\frac{\partial^2\theta_3}{\partial y\partial x}=\frac{xyd}{L_1{}^2\left(L_2{}^2-d^2\right)^{3/2}}$$

$$\frac{\partial^2\theta_3}{\partial x\partial z}=\frac{\partial^2\theta_3}{\partial z\partial x}=\frac{xzd}{L_1{}^2\left(L_2{}^2-d^2\right)^{3/2}}$$

$$\frac{\partial^2\theta_3}{\partial y^2}=\frac{L_1\left(L_2{}^2-d^2\right)+y^2d}{L_1{}^2\left(L_2{}^2-d^2\right)^{3/2}}$$

$$\frac{\partial^2\theta_3}{\partial y\partial z}=\frac{\partial^2\theta_3}{\partial z\partial y}=\frac{yzd}{L_1{}^2\left(L_2{}^2-d^2\right)^{3/2}}$$

$$\frac{\partial^2 \theta_3}{\partial z^2} = \frac{L_1\left(L_2{}^2 - d^2\right) + z^2 d}{L_1{}^2\left(L_2{}^2 - d^2\right)^{3/2}}$$

$$\mathbf{H}_{Bx} = \begin{bmatrix} 0 & 0 & 0 \\ 0 & 0 & 0 \\ 0 & \rho\cos\theta_2 & 0 \end{bmatrix}$$

$$\mathbf{H}_{By} = \begin{bmatrix} 0 & 0 & 0 \\ \sin\theta_1 & 0 & 0 \\ -\rho\cos\theta_1\cos\theta_2 & \rho\sin\theta_1\sin\theta_2 & 0 \end{bmatrix}$$

Spherical space:

$$k_B \hat{N}_B = \frac{\partial \hat{T}_B}{\partial S_S} = \frac{\left[\mathbf{I} - \hat{T}_B \hat{T}_B{}^T\right]}{\left|\mathbf{J}_B \hat{T}_J\right|} \left[\hat{T}_J{}^T \begin{bmatrix} \mathbf{H}_{Bx} \\ \mathbf{H}_{By} \\ \mathbf{H}_{Bz} \end{bmatrix} \hat{T}_J + \mathbf{J}_B k_J \hat{N}_J \right]$$

$$\mathbf{H}_{Bz} = \begin{bmatrix} 0 & 0 & 0 \\ \cos\theta_1 & 0 & 0 \\ \rho\sin\theta_1\cos\theta_2 & \rho\cos\theta_1\sin\theta_2 & 0 \end{bmatrix}$$

where